Creating and Controlling Magnetic Fields to Trap Ultracold Atoms

Hannah Weaver
Jin Group
August 15, 2013
University of Colorado, Boulder – Physics REU

Abstract

The study of ultracold atoms has opened a portal into the world of novel states of matter governed by the laws of quantum mechanics. In particular, strongly interacting fermions at temperatures close to absolute zero respond to magnetic resonances that tune their behavior in the BCS-BEC crossover regime. The construction of a new apparatus designed to study the quantum properties of such strongly interacting Fermi gases is currently underway. The first stage of the experiment utilizes a magneto-optical trap to collect atoms from an atomic vapor source. This project explores the control and stabilization of magnetic fields in this trap using servo feedback electronics. Transfer processes in later stages of the experiment require more precise control of magnetic fields and the preliminary characterizations of a digital servo control for this purpose are reported.

1. Introduction

1.1 A brief history of ultracold atoms

The curious quantum world of the atom becomes apparent when atoms are trapped and studied at very low temperatures where the wavelength of the matter is comparable to the spacing between particles. In this regime, we observe phenomena such as condensation, degeneracy, and strong interactions that shed light on the laws that govern the constituent particles of matter [1, 2, 3]. The first of these behaviors to be detected was a Bose-Einstein Condensate in 1995. Eric Cornell and Carl Wieman observed a collection of bosons, rubidium-87, condense into the same ground state below a certain critical temperature [1]. For their realization, they shared the 2001 Nobel Prize in Physics. A few years later, Deborah Jin's group observed the first degenerate atomic Fermi gas in an ensemble of potassium-40 atoms [2]. This characteristic arises when fermions are cooled to an average temperature below the Fermi temperature and the effects of Fermi-Dirac statistics dominate. In practice, the fermions occupy all of the lowest energy quantum states with exactly one atom in each state as they obey the Pauli exclusion principle. For this reason, the density of the ensemble remains frozen even at very low temperatures. Not long after this discovery, the Jin group created a fermionic superfluid where the atoms are correlated in such a way that they form a pair comprised of a spin-up and a spin-down fermion that acts like a boson [3].

Since this time, scientists have developed ways to tune the interaction strength between atoms using special magnetic resonances. This has opened the door for exploration of a crossover regime between two different kinds of interactions where fermions behave either like tightly bound molecules or weakly correlated Cooper pairs [4]. We hope to continue studying this BCS-BEC crossover regime and other quantum phenomena with our new apparatus.

1.2 The new & improved fermion machine

The construction of the new fermion experiment is still underway, but a schematic of the proposed product is shown in *Fig. 1*. The apparatus boils down to a few key components. The first ingredient is a collection of atoms to study and we choose potassium-40, a stable fermionic alkali metal that is easy to control and characterize because of its hydrogen-like structure. The atomic vapor is produced by a chemical reaction
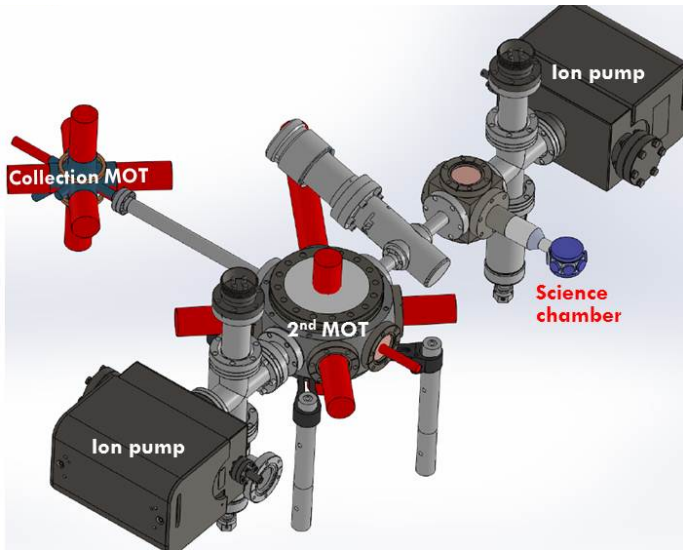
Figure 1: Proposed experimental apparatus. Two MOT chambers intersected by orthogonal laser beams trap and cool atoms to a few nanokelvin. Ion pumps create a low pressure environment of less than 10^{-11} Torr. Atoms are manipulated and imaged in the science chamber.

between an enriched potassium salt and calcium and then loaded into the first collection chamber. The second component is a long hydraulic-stabilized table filled with optics that tune the lasers to a desirable wavelength, power, and polarization. The responsibility of trapping and cooling the atoms rests in the hands of the two magneto-optical traps (MOTs). The first chamber collects the atomic vapor from a room temperature source, and the second chamber further cools the atoms at higher vacuum to achieve longer trapping lifetimes. The scientific mechanism behind the MOT will be explained later in this paper.

This fermion machine is not an entirely new conception but an improvement upon an older apparatus built over ten years ago [5]. In nature, potassium-40 occurs in approximately 0.01% abundance so we use a 14% enriched potassium-40 salt, a fourfold improvement over the old experiment. Additionally in the previous set-up, all imaging and magnetic trapping was performed in the second MOT chamber. By transferring the atoms to a separate science chamber, we will achieve better optical access to the atoms which allows more freedom in the type of experiment we can conduct.

My project this summer begins in the very first stages of the apparatus at the collection chamber. My goal was to characterize the magnetic field here and explore ways of controlling current to tune magnetic fields.

2. The Magneto-Optical Trap

2.1 How it works

A MOT (*Fig.* 2) uses light and magnetic fields to trap atoms and is one of the least expensive ways to cool an atomic cloud to temperatures below 1 mK [6]. Three counter-propagating orthogonal laser beams, reflected back along the same direction, intersect in the center of the trap. All beams are tuned to a slightly lower frequency than the atoms would like to absorb. When the atoms move away from the trap center toward the laser source, they are able to absorb this "red-detuned" light whose frequency is up-shifted by the Doppler Effect. Photons carry a momentum of $\hbar k$ that must be conserved in this atom-photon
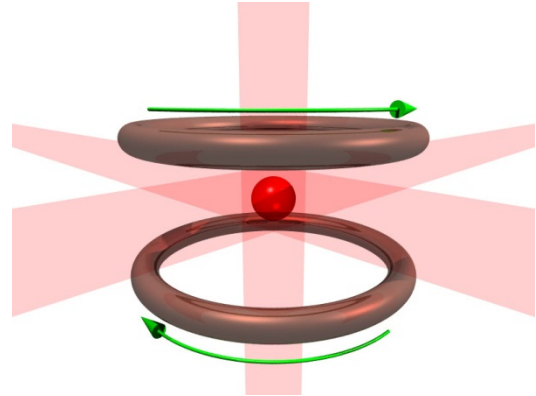

Figure 2: Magneto-Optical Trap (MOT). Current runs through two circular coils in opposite directions creating a magnetic quadrupole field. Three orthogonal counter-propagating lasers that are red detuned intersect in the trap center.

interaction so that the atom is kicked toward the center of the trap and slowed down. The "kick" is really a tiny nudge, but the effect is additive and over time results in a net decrease in the atom's momentum. This trapping and cooling mechanism is velocity dependent, but we also require precise position control of the atoms. This is achieved with a special magnetic field that takes advantage of the Zeeman Effect (*Fig.* 3) and also results in a photon kick toward the trap center.

2

Zeeman splitting is possible in alkali atoms because they carry a magnetic moment, μ, that can interact with an external magnetic field. This field acts like a perturbation to the Hamiltonian in quantum mechanics:

$$H \quad H_0 \quad V_M$$

where H_0 is the unperturbed Hamiltonian and V_M is given by $V_M \quad -\vec{\mu} \cdot \vec{B}$. This perturbation splits

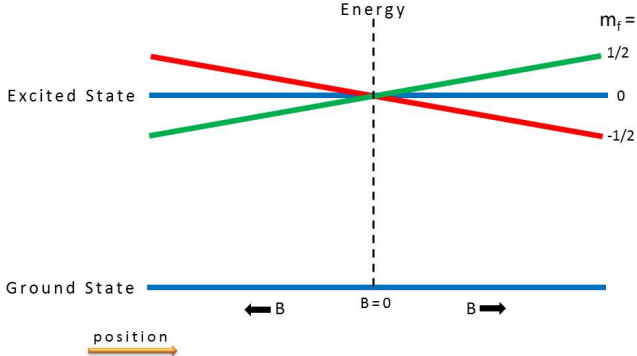*Figure 3:* The Zeeman Effect. In the magnetic quadrupole field of the MOT, the splitting of the excited atomic level increases radially from the trap center such that atoms are able to absorb red-detuned light and experience a kick toward the zero-field center.

the excited atomic level into three magnetic sub-levels where the degree of splitting increases with increasing magnetic field.

The magnetic field that makes this possible is created by two coils separated by their common radius. Running current through the coils in opposite directions creates a magnetic quadrupole field with two important characteristics. The center of the quadrupole field between the coils is zero and the field increases linearly away from here causing the Zeeman splitting within the atom to increase as well. A mathematical description of the exact field of a circular current loop is given in reference [7] and the quadrupole field is a superposition of the field produced by two such coils (see Appendix A).

As an atom moves radially away from the trap center, its atomic resonance is shifted closer to the frequency of the red-detuned photons which the atom can then absorb. After spontaneously emitting a photon and relaxing to the ground state, the atom begins the entire process again as it is successively kicked back to zero-field trap center.

2.2 Characterizing the B-Field

To verify that the vertical and radial components of the MOT field look as the theory predicts, I arrange the two coils of radius 5.5 cm on the optical table aligned 5.5 cm apart and measure the magnetic field along each axis with a
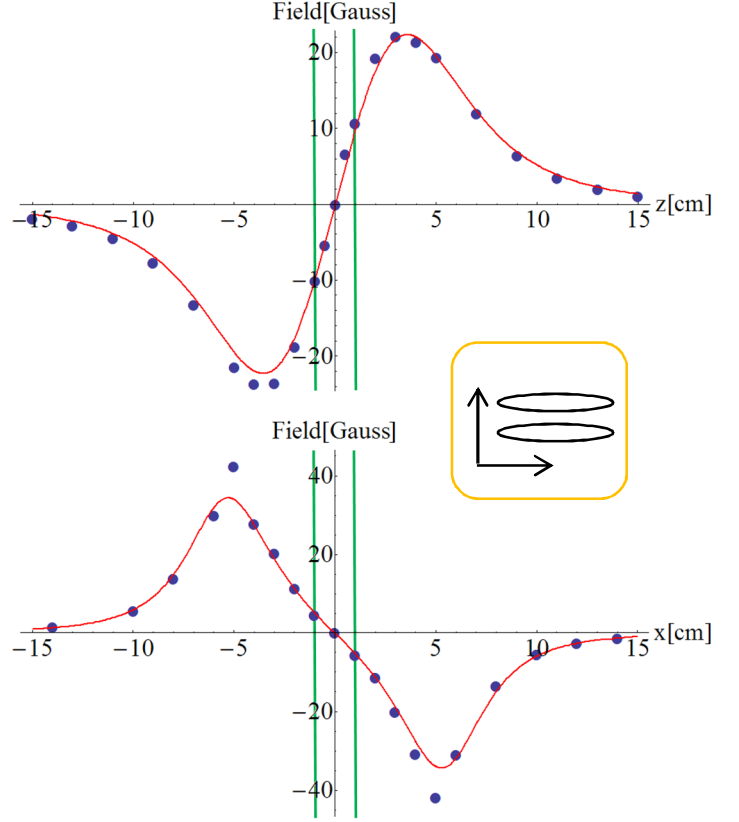
Figure 4: Vertical (top) and horizontal (bottom) component of MOT field measured along respective axes. Green lines mark ± 1 cm of trap center where the atom cloud is contained. Desired field gradients (5 G/cm horizontally and 10 G/cm vertically) are dependent upon the linewidth of the atomic transition excited in the trap.

Gaussmeter. The plots in *Fig. 4* show the measured field components as a function of position along with the theoretical prediction of reference [7] for the given coil parameters. In practice, we are only concerned about the region within 1 cm of the trap center where the atom cloud will be. The important parameter in this region is the gradient of the magnetic field. The gradient we select is determined by the linewidth, (here roughly a few MHz), of the atomic transition excited in the trap. For alkali metals, an applied field of 1 Gauss shifts the atomic transition by about 1 MHz so we require a gradient of 5 G/cm in the radial direction to

3

ensure sufficient splitting of the Lorentz-broadened atomic levels. The gradient is twice as strong in the vertical direction due to the geometry field.

The MOT coils seem to produce a field with the characteristics we desire for the first collection chamber. However, it is also important that the zero-point of the trap center is well controlled so that the atoms can be transferred between chambers in the apparatus with a laser push beam. This control is accomplished with three single current loops or "shim coils".

2.3 Shim coils

The zero-point of the magnetic field in the MOT chamber can be affected by earth's magnetic field or even the optical table. To offset these effects, three shim coils positioned on orthogonal axes around the MOT coils control the position of the quadrupole field center. The field component along the axis of each current loop can be described by the Biot-Savart Law:

$$B_z = \frac{\mu_0}{2} \frac{NIR^2}{(R^2 + z^2)^{3/2}}$$

where N is the number of turns, R is the radis, I is the current, and z is the position along the axis through the coil's center. The number of turns
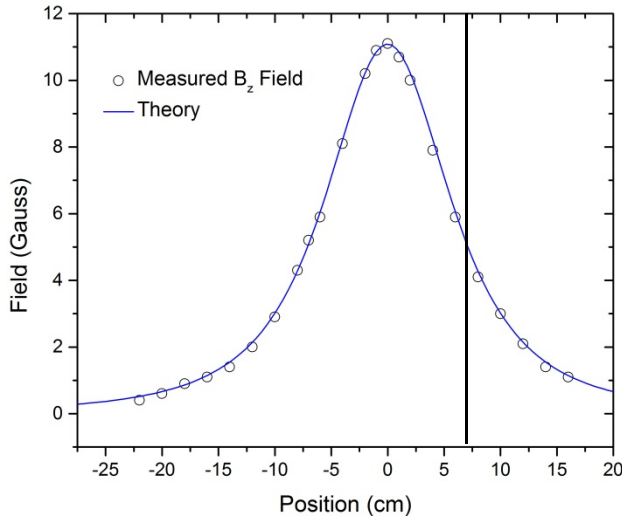

Figure 5: z-component of the shim field as a function of position relative to the coil center for an applied 2 A current. The vertical black line marks the zero-field center of the MOT trap whose position is controlled by three shim coils that exert at most a 5 Gauss field along one axis. The Biot-Savart Law provides the theoretical fit.

(100) and radius (8.5 cm) of the coil are determined by how the loop is constructed. The magnitude of the field is controlled by varying the current between 0-2 Amps. In the experiment, the center of the MOT field will be 7 cm away from the center of the shim coil where the shim field reaches a maximum of 5 Gauss along one axis (*Fig. 5*). By controlling the magnetic fields produced by each coil at the trap center, we control the zero-point of the MOT field.

As atoms are trapped and cooled throughout the experiment, we need to be able to control the field produced by the coils precisely; in order to accomplish this, the current through each coil must be controlled precisely.

3. Current Control

3.1 Field Effect Transistor

The simplest way to control current through any circuit is with a special type of transistor called a Field Effect Transistor (FET). This electronic component is constructed from semiconductor materials and has three elements that are used to control current: the gate, drain, and source. A voltage applied to the gate regulates the conduction of charge carriers, in this case electrons, between the drain and source, effectively controlling the current. An analogy to keep in mind is that the gate voltage on the FET acts like the valve of a water faucet that controls the flow of water, (or current in this case), through the circuit. We use an n-channel MOSFET (IR-2N6764) with a robust current rating for this experiment.
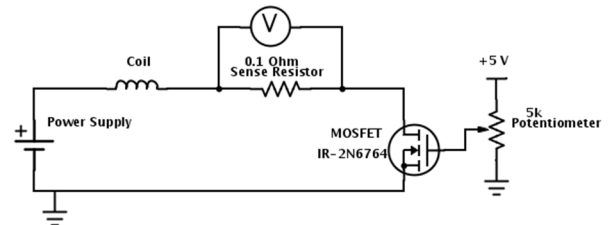

Figure 6: simple FET circuit. Current through the coil is sensed by reading the voltage across a small resistor. A voltage divider controls the gate voltage of the FET.

The circuit used to test the FET is simple (*Fig. 6*). Power is supplied to a coil and the current through the circuit is obtained by reading the voltage across a small sense resistor connected to

the drain of the FET. A voltage divider controls the voltage to the gate and the source is connected to ground.

A plot of the current through the circuit as a function of gate voltage shows how the FET behaves (*Fig. 7*). You might expect that if you turn up the gate voltage by a small amount, the current would increase slightly. But this is not the case. The relationship between current and gate voltage is very nonlinear meaning in order to get any current flow through the circuit, the gate
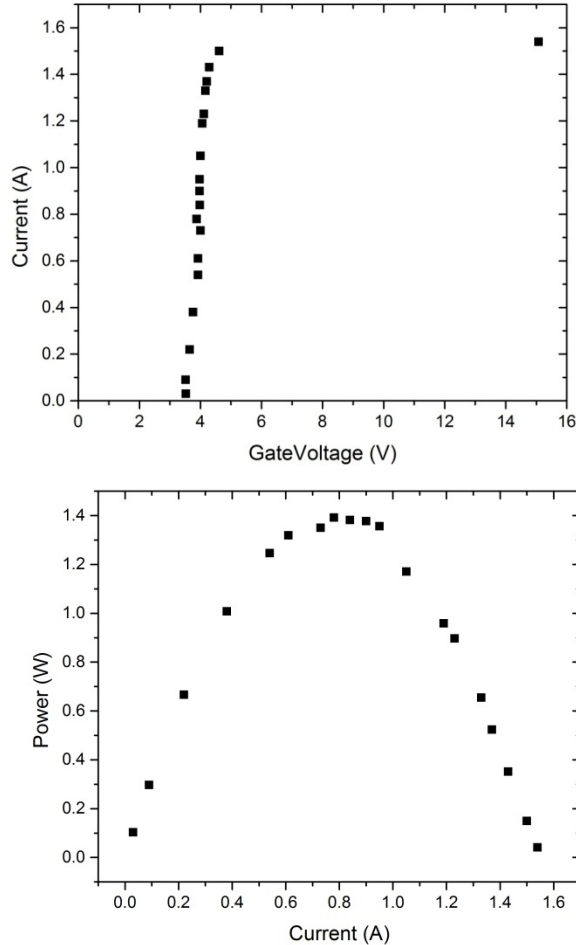
Figure 7: Controlling current with the gate voltage of the FET (top). Current is tuned over a narrow 1 V region before saturation. Power dissipation through the FET (bottom). As resistance across the FET varies, certain values of current cause higher power dissipation which could lead to overheating.

voltage must be above some threshold value at which point the current "blasts on" and quickly saturates. There is only a small region of about a volt over which it is possible to tune the gate voltage to change the current. This is not ideal, but works for many applications.

It is also important to consider power dissipation through the FET because as the gate voltage changes, the resistance between drain and source varies so that for certain values of current and resistance there may be large power dissipation in the FET (*Fig. 7*). To avoid possible heat damage from this effect, all of the FETs in the experiment are mounted on a water-cooled copper board.

In the end, a simple FET is not the best way to control current as there is no feedback system. If the FET heats, for example, the current could drift over time. More complicated electronics in the form of a servo control can stabilize the system.

3.2 Servo control

The feedback control mechanism is analogous to adjusting the amount of water flow through a faucet. There is a quantity you desire to control, water flow through the faucet or current through the circuit. This is the process variable which will be sampled periodically and compared to the set point, the desired water flow or current. The controller ultimately wants to minimize the error between the desired and actual value of the process variable. This is accomplished by adjusting the water valve position or the gate voltage which is called the manipulated variable. In my experiment, the controller, (an operational amplifier or a computer), is constantly measuring and making small adjustments to the current so that it is stable and accurate.

Mathematically, the servo compensates for past, present, and future predicted error using a proportional integral derivative (PID) controller which adjusts the manipulated variable according to the following equation [8]:

$$u(e(t)) = g_P e(t) + g_I \int_0^t e(t) \, dt + g_D \frac{d}{dt} e(t)$$

Here, $u(e(t))$ is the manipulated variable which the servo controls with the signal it outputs, $e(t)$ is the error, and g_P, g_I, g_D are the proportional, integral, and derivative gain, respectively. The gain parameters in large part determine how the servo controls and how the system responds to both analog and digital control mechanisms.
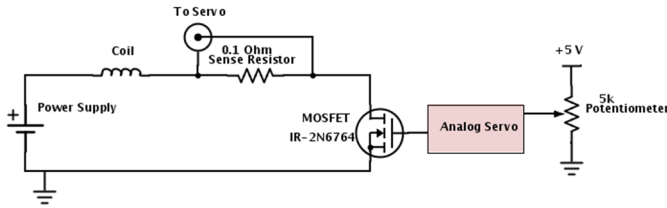
3.2.1 Analog servo control

Figure 8: Simplified FET + analog servo circuit. The servo reads both the voltage across the sense resistor and a voltage from the voltage divider then monitors the current with the voltage it sends to the gate of the FET.

An analog servo is comprised of operational amplifiers, resistors, capacitors, and diodes. The simplified diagram of the circuit is shown in *Fig. 8* while the full diagram of the analog servo used in this project can be found in Appendix B. The servo reads a voltage from the voltage divider at J6 and this signal is input into a follower that uses feedback to ensure the voltage going into the op-amp is exactly what leaves the op-amp. The servo also reads the voltage across the sense resistor at J4 which passes through an amplifier so that the two incoming signals are on the same order of magnitude. The heart of the servo control is in the circuitry surrounding U2. This integrator uses negative feedback to respond to changes in the input voltage over time. If the voltage difference between the two inputs is not zero, the integrator adjusts the output voltage to the gate at J3 that controls the current which should remain steady until the control voltage at J6 is changed. The proportional and integral gains of the servo are set by R7 and C7.

This works well for controlling the current through the MOT and shim coils of the first chamber. However, an analog servo is not a trivial component to assemble and we will need many other servo controls in other parts of the experiment. There is newer computer technology that has the capability to control current more accurately and is also easier to reproduce. Furthermore, the computerized system may be programmed to linearize the relationship between current and gate voltage.

3.2.2 Digital servo control

The digital servo circuit (*Fig. 9*) reads the voltage across a sense resistor and sends a signal to the computer in the form of an analog input. In practice, we also read the voltage across a second resistor in series with the first to see how the system behaves to the output sent to the gate of the FET. The signal from the system is converted from an analog to digital signal which is received by a field-programmable gate array (FPGA). This integrated circuit contains programmable logic components that are wired by a computer to the specifications of the user to form the desired circuit. The FPGA sends out a digital signal in response to the input which is converted back to an analog signal the system can communicate with. Essentially, this forms a large feedback loop
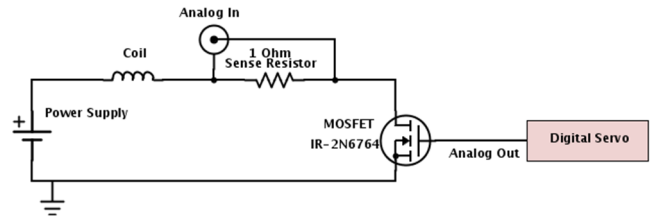

Figure 9: Simplified FET + digital servo circuit. The computer responds to an analog input (a voltage across a small resistor) and controls the current with an analog output to the gate of the FET. The voltage across the second resistor is used to monitor the system's response.

where the parameters of the servo are controlled with a visual code in LabView. For example, with the push of a button, it is possible to change all three gain values – proportional, integral, and derivative– and observe how the system responds to different set points.

Ideally, the bandwidth of the computer should be larger than that of the signal converters (ADC/DAC) which in turn should be larger than the physical system's bandwidth. This guarantees that the servo will be able to maintain control of the system response.

3.3 Servo behavior

3.3.1 Constant set point

First, I investigate the stability of the system in response to a constant current set point when the integral and derivative gains are zero as I increase the proportional gain. *Fig. 10* shows the current through the circuit plotted as a function of time. For low proportional gain, the signal looks a bit noisy, but this is likely measurement noise and only occurs on the order of a part in a thousand. For higher proportional gain, the servo begins to

control faster than the system can respond causing the system to oscillate at a characteristic frequency of about 10 kHz. This is less than ideal behavior, so when precise current control is the goal, we keep the proportional gain relatively low.
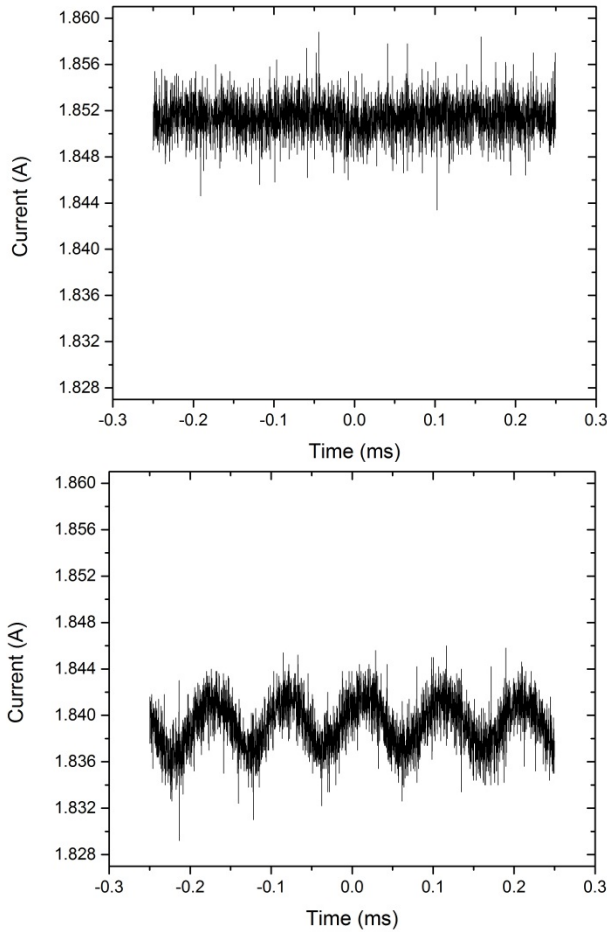

Figure 10: System response to a constant set point of 1.83 A for P=1 (top) and P=4 (bottom). When the proportional gain is small, the system responds well with a steady signal. For larger gain values, the system oscillates at a resonant frequency of approx. 10 kHz as it lags behind in response to the servo control.

3.3.2 Step function set point

Also of interest is how the system responds to a set point that jumps from one current to another for different PID gains. During this process, I maintain the proportional gain at a constant low value and increase only the integral gain. The addition of a derivative gain term could potentially improve the stability of the system, but this term is very sensitive to measurement noise and I found it did not significantly improve
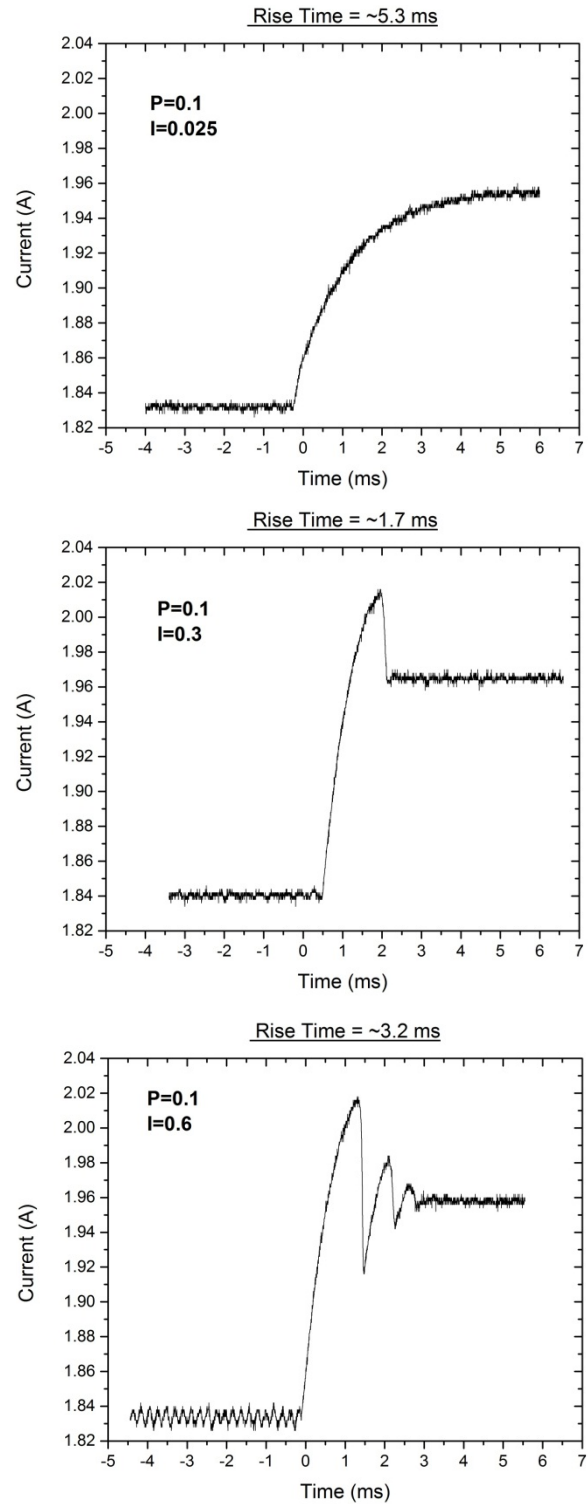

Figure 11: System response to a step function set point from 1.83 A to 1.95 A. Rise to the new set point is slow and smooth for very small integral gain. The system overshoots the step for higher integral gain but responds faster. Oscillations appear for integral gain above this point.

the system's response. Again, I plot the current as a function of time in *Fig. 11* and measure how

long it takes the current to reach the new set point and stabilize. For small integral gain, the system rises smoothly to the new set point but takes quite a while to do so, over five ms. For larger integral gain the rise time is faster, but the system overshoots the set point. For our purposes, this is okay so long as the system is stable after the overshoot. Even larger integral gains cause the system to oscillate. In the end, we require rise times of about half a millisecond during transfer processes. Fall times appear to be much faster, but the fastest rise time achieved by changing PID gains was just under two milliseconds.
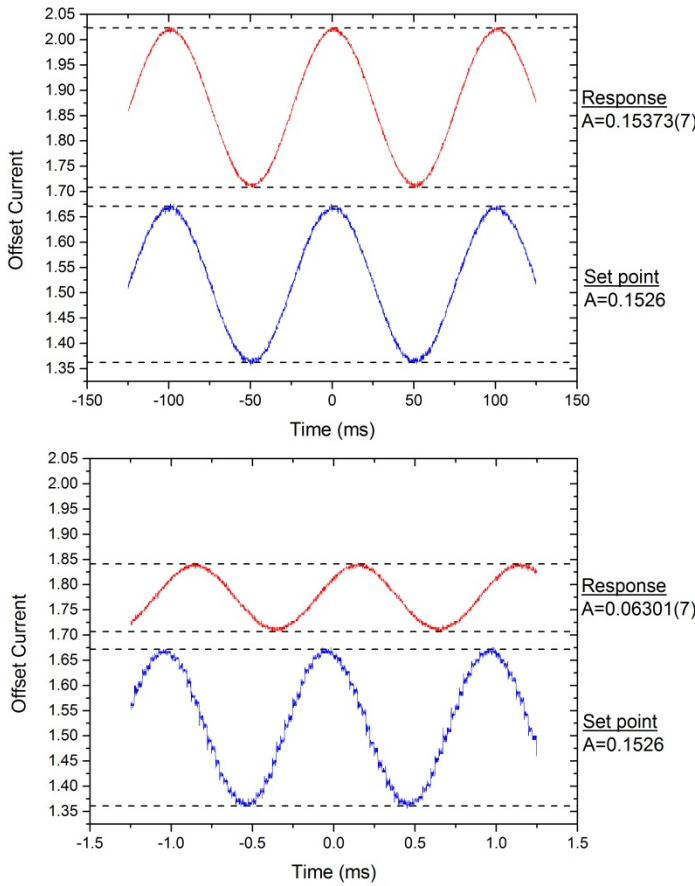
3.3.3 Oscillating set point

Figure 12: System response (**red signal**) to a sine function set point (**blue signal**) at 10 Hz (top, offset 0.35 A) and 1000 Hz (bottom, offset 0.25 A). At low frequencies, the phase and amplitude of the response match the oscillating set point. At higher frequencies, the response lags behind and its amplitude decreases as power is lost in the system.

Finally, I explore the system's behavior when the set point is a sine wave. At low frequencies, I expect the response to match the set point almost exactly without lagging behind. For a sine input
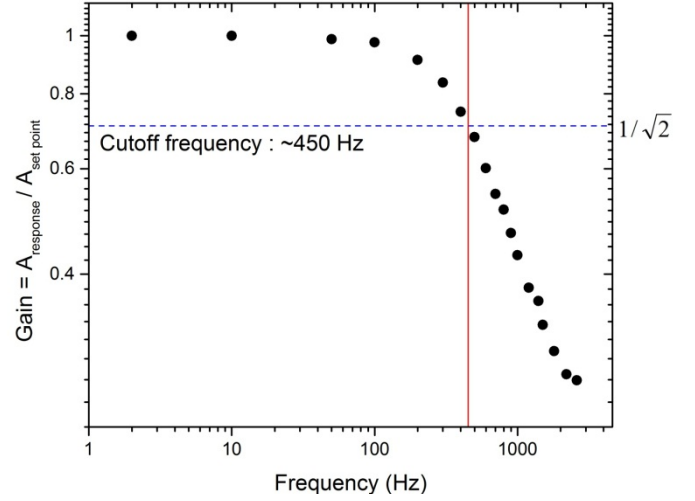

Figure 13: Gain curve for system response to a set point oscillating about 1.5 A. Horizontal dashed line marks half power point. Red vertical line marks cutoff frequency. Note that this is specific to this MOSFET. We can increase the cutoff frequency by using a FET with a larger bandwidth.

of 10 Hz this is exactly what happens (*Fig. 12*). In particular, it is ideal if the amplitude of the response matches that of the set point as this indicates that there is not significant power loss in the signal. With a rapidly oscillating set point at 1 kHz, the system is slow to respond and the amplitude of the response is significantly diminished meaning the energy flow through the system has been reduced. A gain curve (*Fig. 13*) is constructed from the ratio between the response amplitude and the set point amplitude at different frequencies. The horizontal line marks the point where half of the power has been lost as it could not pass through the system. This corresponds to a cutoff frequency of about 500 Hz meaning the system can be safely controlled below this value, (within its bandwidth). It is also important to note that this gain curve is not significantly affected by the PID gains as was the case with the other characterizations. This curve portrays a physical property of the system that depends on each of the electronic components, especially the FET.

4. Future Work

Both analog and digital servos control the current through a coil very well. The analog system will be implemented in the collection MOT while the digital system will be utilized in later parts of the experiment for transferring atoms between MOT and science chambers. Many parameters within

the digital servo have yet to be optimized, most importantly the speed of the servo control and response. It is likely that using a smaller FET could improve the rise and fall time of the servo. In addition, during the transfer process, current will be pulsed through the coil and the servo may need to be optimized for this purpose. Finally, there are many programming capabilities of the FPGA to be explored such as linearization of the relationship between current and gate voltage.

As for the future of the lab, most of the apparatus still needs to be assembled. But the finished product will be a clean, simple, versatile machine for studying ultracold fermions. In particular, it will be used to continue the study of how fermions interact in the BCS-BEC crossover region and how they can be used to model other interesting quantum systems.

5. Acknowledgments

6. References

[1] M.H. Anderson, J.R. Ensher, M.R. Matthews, C.E. Wieman, and E.A. Cornell, Science **269**, 198 (1995).

[2] B. DeMarco and D. S. Jin, Science **285**, 1703 (1999).

[3] C. A. Regal, M. Greiner, and D. S. Jin, Phys. Rev. Lett. **92**, 040403 (2004).

[4] M. Greiner, C. A. Regal, and D. S. Jin, AIP Conference Proceedings, Atomic Physics 19: XIX International Conference on Atomic Physics, Vol. **770**, (2005).

[5] DeMarco, Brian. "Quantum Behavior of an Atomic Fermi Gas." Diss. University of Colorado, Boulder, 2001.

[6] Metcalf, Harold J., and Peter van der Straten. *Laser Cooling and Trapping*. New York: Springer, 1999. 156-164. Print.

[7] Meyrath, Todd. "Electromagnet Design Basics for Cold Atom Experiments." Atom Optics Laboratory Center for Nonlinear Dynamics, University of Texas at Austin, 2003.

[8] College of William and Mary Physics Department. "Chapter 11: Feedback and PID Control Theory." Physics 252 - Electronics I: Introduction to Analog Circuits Lab Manual.

7. Appendix A: mathematical description of a magnetic quadrupole field

The quadrupole field produced by two current carrying coils in an anti-Helmholtz configuration is given by the superposition of a single coil's vertical and radial components [7]:

$$B_z = \frac{\mu NI}{\pi} \frac{1}{\sqrt{(R+\rho)^2 + (z-D)^2}} \left[K(k^2) + \frac{R^2 - \rho^2 - (z-D)^2}{(R-\rho)^2 + (z-D)^2} E(k^2) \right]$$

$$- \frac{\mu NI}{\pi} \frac{1}{\sqrt{(R+\rho)^2 + (z+D)^2}} \left[K(k^2) + \frac{R^2 - \rho^2 - (z+D)^2}{(R-\rho)^2 + (z+D)^2} E(k^2) \right]$$

$$B_\rho = \frac{\mu NI}{\pi \rho} \frac{(z-D)}{\sqrt{(R+\rho)^2 + (z-D)^2}} \left[-K(k^2) + \frac{R^2 - \rho^2 - (z-D)^2}{(R-\rho)^2 + (z-D)^2} E(k^2) \right]$$

$$- \frac{\mu NI}{\pi \rho} \frac{(z+D)}{\sqrt{(R+\rho)^2 + (z+D)^2}} \left[-K(k^2) + \frac{R^2 - \rho^2 - (z+D)^2}{(R-\rho)^2 + (z+D)^2} E(k^2) \right]$$

where

$$k^2 = \frac{4R\rho}{(R+\rho)^2 + (z-D)^2}$$

and $K(k^2)$ and $E(k^2)$ are the complete elliptic integrals for the first and second kind, respectively.

The coordinates (ρ, z) of each coil are defined in cylindrical space where D is the separation between coils (*Fig. 14*).
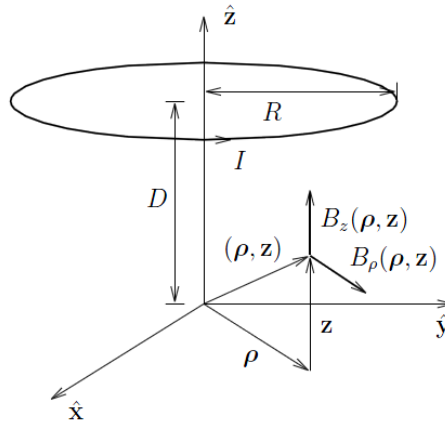

Figure 14: cylindrical coordinates for the magnetic field of a single current carrying loop centered about the vertical z-axis. (Figure borrowed from [7]).

8. Appendix B: analog servo circuit diagram

Note: We use a 20 kΩ resistor at R6 so that signals leaving U4 and U1 can cancel at U2.